Postprint of: Czaja Z., A diagnosis method of analog parts of mixed-signal systems controlled by microcontrollers, Measurement, Vol. 40, Iss. 2 (2007), pp. 158-170, DOI: 10.1016/j.measurement.2006.07.015

A diagnosis method of analog parts of mixed-signal systems controlled by microcontrollers

Zbigniew CZAJA*

Gdansk University of Technology, Faculty of Electronics, Telecommunications and Informatics, Department of Metrology and Electronic Systems, ul. G. Narutowicza 11/12, 80-952 Gdansk, Poland

Abstract

A new class of *K*-D fault diagnosis methods of analog parts in embedded mixed-signal microsystems based on microcontrollers is presented. The methods consist of three stages: a pre-testing stage of a fault dictionary creation, a measurement stage based on the measurement of voltage samples of the time response on a stimulating square impulse of the analog part realized by internal resources of the microcontroller and a fault detection and localisation stage performed by the microcontroller. The fault dictionary in the form of identification curves in the *K*-dimensional space is converted and placed in the program memory of the microcontroller. These methods have the following advantages: measurements of analog parts can be made using only internal resources of popular microcontrollers, the diagnosis procedure does not require big computing power and the codes of its procedure with the fault dictionary do not occupy much space in the program memory of the microcontroller.

Keywords fault diagnosis method, electronic embedded systems, microcontrollers

1. INTRODUCTION

Growing interest in fault diagnosis of analog parts of mixed-signal electronic systems is caused by fast development of the telecommunications, multimedia and automobile markets which base on mixed-signal embedded systems. A lot of these systems have hard-tested analog parts. Hence, new methods of testing or self-testing of

* Corresponding author. Tel.: +48-58-347-14-87; fax: +48-58-347-22-55.
E-mail address: zbczaja@pg.gda.pl

analog parts of these systems, which decrease test cost and guarantee high quality of products, should be developed.

At present, a test of electronic packages using standard testers, which needs access to measurement points on printed boards, becomes impossible. It is caused by the density of packing of elements on printed boards, growth of complexity of circuits in chips, using new types of packages of the chips (e.g. BGA). Hence electronic systems and chips are more often provided with units which enable to test them by themselves. In this aim, an additional block (or blocks) called Built-In Self-Test (BIST) is built-in in the systems or the chips. To test the chip it is introduced into a self-test mode. In this mode the standard function of the chip is turned off, and the BIST is activated. It tests the core of the chip and also its surrounding circuits. For instance, for introducing and controlling of digital circuits working in the self-test mode the bus JTAG (IEEE 1149.1) was elaborated.

Self-testing of analog parts is very difficult and not standardized, because analog circuits are very varied and they are used in various applications. In addition, the offered BISTs are dedicated only for selected, non- numerous classes of circuits, e.g.: adc-BIST for analog to digital converters [1,2,3], BISTs for fully differential circuits [4], BISTs based on the oscillation-test methodology for active analog filters [5,6,7], BISTs for opamps [8]. The feature of these BIST, which increases their production costs, is hardware excess. Hence, development of new methods simplifying the structure and design of BISTs, which allows to decrease costs, is needed.

Often simple electronic embedded systems controlled by microcontrollers consist of not only a digital part, used for control and data processing, but also an analog part mostly used for adjustment of input signals e.g. from sensors. So, to decrease the test cost, it is proposed to use the microcontroller mounted in the system, particularly its hardware resources (used to generate test signals and measure the responses of analog parts) and computing power (used to control a measurement procedure and for computations required by fault detection and localisation procedures), to realize the BIST [9,10,11]. In this way we obtain a reconfigurable BIST. It is created only during the self-testing time. Apart from this time, the microcontroller and its internal devices perform normal functions. Hence, we considerably decrease the number of elements of the BIST which have to be added to the system.

For this task, a new class of fault diagnosis methods which enables fault detection and localization of single parametric (soft) faults of passive components of analog circuits, was elaborated [9]. The originality of the methods is as follows (Fig. 1):

- stimulation of the tested analog part by a square impulse with programmable duration time generated by the microcontroller,
- measurement of K samples u_1, u_2, .., u_K of voltages of the time response of the analog part to a square impulse by the internal Analog to Digital Converter at precise moments t_1, t_2, .., t_K established by the internal timer of the microcontroller,
- the fault detection and the localization realized by the microcontroller based on a measurement result, a fault dictionary and a diagnosis procedure located in its program memory.

2. DESCRIPTION OF THE METHODS

The diagnosis procedure of the methods consists of three stages [9]. In the first pre-testing stage realized only one time for the given analog part, a fault dictionary in the form of a family of identification curves in the multidimensional space (K-dimensional space) is generated in a simulated way on a PC computer. Next, it is converted and placed in the program memory of the microcontroller mounted in the embedded system.

In the second stage, based on internal resources of the microcontroller, the analog part is stimulated by a square impulse with programmable duration time, and K samples of voltage of the time response of the analog part to this square impulse are measured.

In the third stage the microcontroller bases on the measurement result in the form of a measurement point P_m and the fault dictionary performs fault detection and localization. The computations base on an approach described in [12,13], where the measurement point P_m was placed into the map with a family of identification curves (e.g. Fig. 4). Next, the faulty element was localized by location of the P_m point on a particular curve.

Two last stages are realized by the BIST configured from the internal resources of the microcontroller.

2.1. The idea of the methods

It was tested, in a simulating and practical way, that the responses of a linear electronic circuit to a square impulse for the assumed range of change of values for different elements do not fall on each other [9], as shown in Fig. 2. This figure presents three sets of time responses of the circuit to the square impulse, shown in Fig. 6. Each set represents changes of the response of the circuit following from changes of the value of the given element (e.g. C1) with the assumption that the remaining elements have nominal values. These changes are represented as ratio $p_i/p_{i\ nom}$ (*value of the i-th element / nominal value of i-th element*). Therefore it is possible to discern and to assign these responses to given elements (to assign the set of time responses to the given element) and to their given values (to discern the individual response in the set).

If we make cross-sections of Fig. 2 at moments t_1 and t_2 (for clarity, the moment t_3 was omitted) along the co-ordinate $p_i/p_{i\ nom}$, we obtain the charts shown in Fig. 3. Hence, we can say that particular curves in this figure represent changes of temporary values of voltage of time response at the moment t_1 (continuous lines) and at the moment t_2 (dotted lines) in function of changes (deviations) of values of particular elements. Hence, the curves represent deviations of values of elements. They are separated and all cross in the nominal point for which all elements have nominal values – the circuit is fault-free. So, they can be helpful in a fault diagnosis. For this purpose they were converted in the following way.

It was assumed that the voltage sample (the temporary value of the voltage) of the response of the circuit at a moment t_1 (u_1) is the first co-ordinate, the voltage sample at the moment t_2 (u_2) is the second one and etc. Successively changing the value of a particular element p_i (where i=1,..,I, I - the number of elements of the analog part) from $0.1p_{i\ nom}$ to $10p_{i\ nom}$ ($p_{i\ nom}$ - the nominal value of i-th element), the particular curves l_i are drawn in the K-dimensional (K-D) space. In this way, to draw curves for all elements, we obtain a family of identification curves shown in Fig. 4 for K=2 [10] and in Fig. 5 for K=3 [11].

Fig. 4 was created directly from Fig. 3. This approach enables to integrate the two curves (continuous and dotted lines) of the particular elements into one. The first co-ordinate U_1 (Fig. 4) fits the changes of the co-ordinate U (Fig. 3) of curves $U_1(\cdot)$

(continuous lines) and the second one U_2 fits the changes of the co-ordinate U of curves $U_2(\cdot)$ (dotted lines) for the full range of changes of values of elements. Therefore values of the elements can be represented only by a scale of the curve (see the C1 curve).

Fig. 5 is an extension of Fig. 4 based on an addition of third co-ordinate U_3 representing changes of temporary values of the voltage of the time response at the moment t_3.

We can present the above operation in the form of the transformation [9]:

$$T(p_i) = \sum_{k=1}^{K} u(p_i, t_k)\mathbf{i}_k , \tag{1}$$

where: $\mathbf{i}_k$ - is a versor of a k-dimension, k=1, .., K, K – the number of samples, $u(p_i,t_k)$ – value of the voltage sample at the moment t_k for a change of values of the element p_i.

The transformation (1) maps changes of values of p_i elements into the identification curves l_i in the K-D space. For K=2 the curves are placed on a plane (the 2-D method) [10] and for K=3 in the 3-D space (the 3-D method) [11].

So we can describe the family of identification curves as a set of transformations $T_I = \{T(p_i)\}_{i=1, \ldots, I}$. It establishes the fault dictionary of the circuit for which it was drawn. The curves cross over at a point named the nominal point P_{nom} for which the circuit is fault free, and the particular curve l_i represents a deviation of value of the p_i element.

The location and shape of the curves depend exclusively on the duration time of the stimuli and the probe moments. So it is very important to determine these parameters.

2.2. Assignment of duration time of the stimulant square impulse

We assumed that the stimulant square impulse is generated at the digital output of the microcontroller [9,10,11]. Because the amplitude of the stimulus U_{IN} is *a priori* set to the supply voltage of the digital part, we can fit only the duration time T of the stimulant square impulse to obtain the best shapes of the time responses. It enables to obtain possibly the best lay-out of the curves in the space for the fault detection and localization.

For all classes of the *K*-D methods the duration time of the stimulant square impulse is assigned in two steps [9]. In the first step this time is set to a value $T = 1/f_c$, where f_c is the cut-off frequency of the analog part (Fig. 6). In the second one we assign the maximum value of the output signal $U_{OUT}=\xi \cdot U_{IN}$ for the nominal values of elements of the circuit, where coefficient $\xi \in < 0, 1 >$. Next we fit the duration time T in a simulated way to obtainment of a given maximum value U_{OUT} of the output signal. The Fig. 7 shows the input stimulant signal u_{IN} (T=25μs) and the response signal u_{OUT} of the nominal circuit for $\xi = 1$.

2.3. Assignment of moments of voltage samples

The fault diagnosis methods require exact determination of *K* moments t_1, t_2 and t_K of voltage samples of the response signal. The location and shape of the curves exclusively depend on these moments. So they should be chosen in a way enabling the best localization resolution of the faults. Thus, the identification curves should have similar length, and they should be as distant between themselves as it is possible. Based on these assumptions and results of simulation, investigations were elaborated on the criteria and the procedure of determination of the moments of voltage samples.

The way of determination of moments of voltage samples depends on the number *K* of voltage samples. So, it is different e.g. for the 2-D method and for the 3-D method.

For the 2-D and 3-D methods the size of the fault dictionary is small, hence they can be used in practice e.g. as self-testing methods of the embedded systems. So, for these methods the determination of moments of voltage samples is described exactly.

For the 2-D method two moments t_1 and t_2 are determined based on criteria of the best localization resolution of identification curves on a plane [11].

It is known, that the response of the tested circuit consists of two steps (see Fig. 7):

- accumulation of energy (loading of capacitors) during the duration of the stimulant signal (0, T),
- emission of energy (discharging of capacitors) after the stimulant signal, during (T, νT) time (where $\nu = 1, 2, ..$ establishes the observation time).

Therefore, we observe two different behaviors of the circuit. Moment t_1 is determined in the first step $t_1 \in (0, T)$, and the moment t_2 in the second one $t_2 \in (T, \nu T)$.

To determine the moments t_1 and t_2, for which we obtain the best localization resolution, a coefficient of the localization resolution λ_i of the p_i element was introduced [11]. It is defined in the following way:

$$\lambda_i(t_k) = \max_{j=1,..,J}\{u(p_{ij},t_k)\} - \min_{j=1,..,J}\{u(p_{ij},t_k)\}, \tag{2}$$

where J – the number of values of the element p_i in the range from $0.1p_{i\,nom}$ to $10p_{i\,nom}$, each l_i curve is represented by a set of J q_{ij} points ($T(p_{ij}) \rightarrow q_{ij}$), t_k – the moment of the k-th sample, $k = 1, .., K$ and $t_k \in (0, \nu T)$, K – the number of samples.

This coefficient describes the difference between the maximum and minimum value of voltage of the circuit responses at the moment t_k for a defined range of changes of values of the p_i element.

The coefficient λ has the form:

$$\lambda(t) = \frac{1}{I}\sum_{i=1}^{I}\frac{\lambda_i(t)}{\max\limits_{k=1,..,K}\{\lambda_i(t)\}} \tag{3}$$

The coefficient λ is the average value of the normalized coefficients λ_i, then its maximum value represents the optimum sensitivity of the circuit response to changes of values of all elements. Thus we can define:

$$\lambda_{max\,1} = \max_{k=1,..,K1,\ t_k\in(0,T)}\{\lambda(t_k)\} \tag{4a}$$

and

$$\lambda_{max\,2} = \max_{k=K1,..,K,\ t_k\in(T,\nu T)}\{\lambda(t_k)\} \tag{4b}$$

where $K1$ – the number of samples for the time range $(0, T)$.

So, the solutions of (4) determines the two moments of voltage samples:

$$\lambda_{max1} \rightarrow t_1 \quad \text{and} \quad \lambda_{max2} \rightarrow t_2 \tag{5}$$

Fig. 8 shows charts of all coefficients λ_i and the coefficient λ. for the analog part (Fig. 6). It is seen that in the first step (loading of capacitors) the properties of the circuit significantly depend on the values of R1 and C1 elements. However, in the second step (discharge of capacitors) the values of the capacitor C2 mainly influences the form of identification curves.

For the analog part (Fig. 6) the following moments of voltage samples t_1 = 14.8μs and t_2 = 33.6μs were determined [11]. For these moments, identification curves on the plane U1, U2 are drawn in the Fig. 3.

The 3-D method uses moments t_1 and t_2 determined for the 2-D method. Thus, for the 3-D method only the moment t_3 is additionally assigned. It determines the third co-ordinate U3 of the measurement space with the family of the identification curves. It bases on the criteria of an additional increase of the localisation resolution [11].

Assignation of moment t_3 of the voltage sample can be realized in many ways depending on established criteria. The following criteria were elaborated:

- maximum difference of time between t_3 and t_1 and between t_3 and t_2,
- improvement of identification accuracy of l_i identification curve, where the curve can be chosen by us or it can be the shorter curve,
- improvement of localisation resolution by drawing aside neighboring curves chosen by us or neighboring curves placed too close to each other.

The first criterion [11] assures maximum difference among moment t_3 and moments t_1 and t_2 . It allows the observation of the response signal at the moment when the signal is maximally different. It ensures getting out maximum information from the response signal by the third sample at the t_3 moment.

At the beginning of determination of the moment t_3 the maximum values of coefficients λ_i for all p_i elements are calculated:

$$\lambda_{i1} = \max_{k=1,..,K1,\ t_k \in (0,T)} \{\lambda_i(t_k)\} \tag{6a}$$

and

$$\lambda_{i2} = \max_{k=K1,..,K,\ t_k \in (T,vT)} \{\lambda_i(t_k)\} \tag{6b}$$

Based on these coefficients the moments of samples are assigned:

$$\lambda_{i\,1} \rightarrow t_{i\,1} \quad \text{and} \quad \lambda_{i\,2} \rightarrow t_{i\,2} \tag{7}$$

Next the maximum difference among moment t_3 and moments t_1 and t_2 is appointed:

$$\Delta t_3 = \max\{\max_{i=1,..,I}\{|\,t_1 - t_{i1}\,|\}, \max_{i=1,..,I}\{|\,t_2 - t_{i2}\,|\}\} \tag{8}$$

If $\max_{i=1,..,I}\{|\,t_1 - t_{i1}\,|\} > \max_{i=1,..,I}\{|\,t_2 - t_{i2}\,|\}$ then $\Delta t_3 \rightarrow t_3 = t_{i1}$, else $\Delta t_3 \rightarrow t_3 = t_{i2}$.

For the tested circuit (Fig. 6) the moment t_3 of third sample is equal to 59.2μs [11] and it represents the moment at which the coefficient λ_{C2} has its maximum value (see Fig. 8). Thus the l_{C2} curve of the C2 element is more distinguished then the other ones (compare Fig. 4 and Fig. 5). But also the distances among all identification curves are greater. So, moving the identification curves from the plane to the 3-D space improves the fault localization resolution.

The second criterion [9] of improvement of identification accuracy of the i-th identification curve for the 3-D method bases on an extension of the length of the curve.

We can lengthen the l_i curve chosen by us. In this case $t_3 = t_{i\,max}$, where $\lambda_{i\,\max} \rightarrow t_{i\,\max}$:

$$\lambda_{i\,\max} = \max_{k=1,..,K \text{ i } t_k \in (0,vT)} \{\lambda_i(t_k)\} \tag{9}$$

To improve the localization resolution this criterion is applied to lengthen the shorter l_i curve. Because the l_i curve of the p_i element is represented by the set of points $\{q_{ij}\}_{j=1,..,J}$, the length h_i of the l_i curve can be calculated from the following form:

$$h_i = \sum_{j=1}^{J-1} \sqrt{\sum_{k=1}^{K} (u_{ij}^k - u_{i(j+1)}^k)^2} \tag{10}$$

where: $u_{ij}^k = u(p_{ij},t_k)$. – k-th co-ordinate of the q_{ij} point.

After calculation of all h_i lengths it determines the shorter curve and the moment t_3:

$$h_{\min} = \min_{i=1,..,I}\{h_i\}, \quad h_{min} \rightarrow i \text{ and } t_3 = t_{i\,max}. \tag{11}$$

The third criterion [9] of improvement of localization resolution has two variants. In the first variant the neighboring curves chosen by us are drawn aside. In the second, neighboring curves placed too the closest to each other are chosen for this operation.

In the first case we choose two neighboring curves l_r and l_s, where: $r < s$ and r=1,..,I s=2,..,I. The coefficient $\gamma_{\max}^{rs}$ of the difference between responses of the circuit for a change of p_r and p_s elements at the moment t_k is assigned:

$$\gamma_k^{rs} = \sum_{j=1}^{J} \left| u(p_{rj},t_k) - u(p_{sj},t_k) \right| \tag{12}$$

Next the maximum value of this coefficient is determined:

$$\gamma_{\max}^{rs} = \max_{k=1,..,K \text{ and } t_k \in (0,vT)} \{\gamma_k^{rs}\} \tag{13}$$

Hence $\gamma_{\max}^{rs} \rightarrow k \rightarrow t_k . \rightarrow t_3$.

Determination of neighboring curves placed too close to each other is realized the following way:

Each l_i curve is partitioned on two curves l_{i1} and l_{i2} in relation to the nominal point:

- the l_{i1} curve is drawn for changes of values of p_i element from 0.1 to 1 $p_{i\,nom}$.
- the l_{i2} curve is drawn for changes of values of p_i element from 1 to 10 $p_{i\,nom}$.

So we have for consideration $2I$ curves, what gives $C_{2I}{}^2$ pairs of curves and $2I$ pairs of neighboring curves.

The coefficient of localization resolution between l_r and l_s curves can be defined (Fig. 9) as:

$$\chi_{r_1 s_1} = \frac{S_{r_1 s_1}}{h_{r_1 s_1}} \tag{14}$$

where: $S_{r_1 s_1}$ is the magnitude representing the area between l_{r1} and l_{s1} curves. $h_{r_1 s_1}$ - length of surface $S_{r_1 s_1}$. It is assumed that $h_{r_1 s_1}$ is the average value of lengths of l_{r1} and l_{s1} curves. Hence:

$$h_{r_1 s_1} = \frac{h_{r_1} + h_{s_1}}{2}, \tag{15}$$

and:

$$h_{i_1} = \sum_{j=1}^{j_{nom}-1} \sqrt{\sum_{k=1}^{K} (u_{ij}^k - u_{i(j+1)}^k)^2} \tag{16a}$$

and

$$h_{i_2} = \sum_{j=j_{nom}}^{J-1} \sqrt{\sum_{k=1}^{K} (u_{ij}^k - u_{i(j+1)}^k)^2} \; . \tag{16b}$$

where j_{nom} is the index for which $p_{i\,j\,nom} = p_{i\,nom}$.

To simplify calculations of the area of the surface $S_{r_1 s_1}$ the following relationship was assumed:

$$S_{r_1 s_1} = \sum_{j=1}^{j_{nom}-1} \sqrt{\sum_{k=1}^{K} (u^k_{r_1 j} - u^k_{s_1 j})^2} \tag{17a}$$

and

$$S_{r_2 s_2} = \sum_{j=j_{nom}+1}^{J} \sqrt{\sum_{k=1}^{K} (u^k_{r_2 j} - u^k_{s_2 j})^2} \tag{17b}$$

So, first the distances between points $q_{r_1 j}$ and $q_{s_1 j}$ of l_{r1} and l_{s1} curves respectively are calculated. Next they are summed. Because J is a constant for all curves, the coefficients $S_{r_1 s_1}$ reflects the surface area included between the l_{r1} and l_{s1} curves.

The minimum value of coefficients of localization resolution $\chi_{r_1 s_1}$ and $\chi_{r_2 s_2}$ of the l_{r1} and l_{s1} neighboring curves points to curves, which are placed too the closest to each other:

$$\chi_{nim} = \min_{r=1,..,I,\, s=2,..,I,\, r<,s} \{\chi_{r_1 s_1}, \chi_{r_2 s_2}\}. \tag{18}$$

So, χ_{min} points to the pair of l_r and l_s neighboring curves.

Next, moment t_3 is determined as described in the first variant of this criterion (based on (12) and (13)).

For K-D methods, where $K > 3$, two ways of determination of moments of voltage samples are proposed [9]:

- even location of K moments t_k in $(0, \nu T)$,
- chosen at I moments t_k in $(0, \nu T)$, where $t_k = t_{i\,max}$, where $\lambda_{i\,\max} \rightarrow t_{i\,\max}$,
- chosen at $2I$ moments t_k in $(0, \nu T)$, where $t_k = t_{i\,1\,max}$, $\lambda_{i\,1\,\max} \rightarrow t_{i\,1\,\max}$, $t_{k+1} = t_{i\,2\,max}$, $\lambda_{I\,2\,\max} \rightarrow t_{i\,2\,\max}$.

In the first case we choose the number K and calculate the moments $t_k = (\nu T / K) \cdot k$. The size of the fault dictionary is equal to $I \cdot J \cdot K$, so its linearity depends on the number K. Also, when $K \rightarrow \infty$ then $t_k - t_{k+1} \rightarrow 0$ and the same $u_{ij}^k - u_{ij}^{k+1} \rightarrow 0$. Hence increasing of the number K is not profitable. The size of the fault dictionary and the computing complexity grow faster, than the fault localization resolution. Taking this fact into consideration, the number K should be as small as possible e.g. K=2 or K=3.

If the size of the fault dictionary is not limited, it is good to use the second or third way of determination of moments of voltage samples. In these cases the number K depends on the number I of elements, which is profitable, because increasing the number I makes the fault localization resolution worse (thickens the map of identification curves). So proportionally increasing the number K keeps the fault localization resolution at the required level.

3. THE DIAGNOSIS PROCEDURE OF THE METHOD

As described at the beginning of the previous paragraph, the diagnosis procedure consists of three stages:

- the pre-testing stage of creation of a fault dictionary,
- the measurement stage,
- the fault detection and localization stage.

The first stage is realized during the design of the system and only one time for the given analog circuit in a simulated way on a PC. The remaining stages deal with self-testing of the analog part of the system executed by the BIST configured from internal resources of the microcontroller.

3.1. The creation of the fault dictionary

With regard to the limited size of the program memory of the microcontroller, which is destined mainly for a program controlling the embedded system, the fault dictionary should have the smallest size while keeping an adequate level of location resolution. For that reason, from the proprieties of the 8-bit microcontrollers and simulation tests the following assumptions result [9]:

- The l_i identification curve of the p_i element is represented by a set of points $\{q_{ij}\}_{j=1,..,J}$, which are calculated from the set of values of elements $\{p_{ij}\}$ and equally placed on this curve.
- Each q_{ij} point has K 8-bit co-ordinates (u_{1ij}, u_{2ij}, u_{3ij}, .., u_{Kij}). That is voltages u_{kij} are signified in binary code according to a format of a conversion result of the Analog

to Digital Converter (ADC) of the microcontroller. So $u_{kij}[\mathrm{V}] = \frac{u_{kij}[\text{binary code}]}{2^8 - 1} \cdot V_{cc}$, where V_{cc}=5V.

- A nominal point q_{nom} and a coefficient ε_{nom} [14] which represents the size of a nominal area represent a fault-free circuit.

So, we can describe the fault dictionary in the following way: $S_{IJ} = \{(u_{1ij}, u_{2ij}, u_{3ij}, .., u_{Kij}), (u_{1nom}, u_{2\,nom}, u_{3\,nom}, .., u_{K\,nom}), \varepsilon_{nom}\}_{i=1,..,I,\, j=1,..,J}$.

Hence, each curve is described by $J{\cdot}K$ bytes. It gives a fault dictionary with the dimension $I{\cdot}J{\cdot}K + K + 1$ bytes. When K=2 or K=3 (I=4, J=32) it is small (259 or 388 bytes) in relation to the size of the program memory of a typical 8-bit microcontroller (e.g. ATmega16 has 16kB of FLASH memory).

The fault dictionary is generated on a PC computer using the Matlab program [9]. For the assumed range of changes from 0.1 $p_{i\,nom}$ to 10 $p_{i\,nom}$ the values of respective elements are chosen using the logspace function. It gives as far as possible an equal location of approximation points q_{ij} on l_i identification curves. For all values p_{ij} of each p_i element (remaining elements have nominal values), simulation of the time response of the analog part to a square impulse with the same parameters (T, t_1, t_2 , .., t_K) which the real impulse at the input of the CUT (Fig. 6) is performed using the Control Toolbox. Only variables are stored there which represent voltage values of the responses at moments t_1, t_2, .., t_K. Next, the fault dictionary S_{IJ} created in this way is written to a text file using function dlmwrite, and it is converted and placed into the file with the full code of a program. Next this file is compiled to Intel-HEX file. In the last step the microcontroller is programmed in the ISP mode.

3.2. The measurement procedure

The measurement procedure is realized by the BIST consisting only of internal resources of the microcontroller:

- the timers determine the duration time of the stimuli and moments of voltage samples,
- the ADC measures the instantaneous value of the voltage of the response signal.

This procedure is illustrated on the example of a system controlled by the Atmega16 [15] microcontroller (Fig. 6). This 8-bit microcontroller has advanced two 8-bit timers/counters (Timer 0 and Timer 2) and one 16-bit timer/counter (Timer 1) enabling precise measurement of time, counting of external pulses, generating programmed square impulses and it has the 10-bit SAR-type ADC with a sample & hold circuit which enables the measurement of instantaneous values of voltage.

Fig. 10 illustrates only an idea of the measurement of K voltage samples. The real measurement procedure taking into account the long conversion time of the ADC is shown in Fig. 11.

From Fig. 10 it is seen that [9] Timer 0 controls the duration time of the stimulant square impulse on line OC0 connected to the input of the tested analog circuit. Timer 1 is responsible for counting of moments t_k of auto triggering of the ADC.

In the first step the tested circuit is introduced into an initial state. It was assumed that it takes about $5T$. Next a square impulse with duration time T counted by Timer 0 is generated on the OC0 line. The way of impulse generation does not depend on the number K, so it is the same for all methods.

When generation of the square impulse starts, Timer 1 is started to count time t_1. The overflow of Timer 1 auto triggers the ADC which measures sample $u_{1\,m}$, and loads value t_2 to Timer 1 and again starts the Timer 1. It is repeated K times. In the end we obtain a measurement point P_m with co-ordinates ($u_{1\,m}$, $u_{2\,m}$, $u_{3\,m}$, .., $u_{K\,m}$).

In practice we have to consider the long conversion time of the ADC. This time (minimum 65μs) is greater than the duration time of the stimuli (25 μs). So, the measurement procedure was partitioned into K parts (Fig. 11). In each part, after about $5T$, the analog circuit is stimulated by the square impulse with duration time T counted by Timer 0 and only one sample u_{kij} is probed by the ADC at moment t_k. This moment is determined by the Timer 1 always in relation to the beginning of the stimuli.

This solution lengthens only the time of the measurement. It does not influence the size of the code of the measurement procedure because each part is realized by the same function called K times with a different parameter t_k. The flowchart of this function is shown in Fig. 12.

The measurement of one sample $u_{k\,m}$ function is called with the variable *data_k* (Fig. 12). It contains a value corresponding to time t_k. The function returns in this

variable the value related to the voltage $u_{k\ m}$, which is written to a table of variables *um*[*K*] by the main measurement function. The variable *end_conv* is used to sync between the main function and interrupt services of autonomic simultaneously running with core processor peripherals. In the first step of the function values are loaded to Timer 0 and Timer 1. Next Timer 0 starts in a normal mode with the disabling overflow interrupt. After time 5T, a stimulus is generated at output OC0 and the following are started: Timer 0 in the clear timer in compare match (CTC) mode with clear OC0 in compare match to count *T* and Time 1 in normal mode to determine time t_k. Next the function waits for the finish of the ADC conversion.

Because the ATmega16 microcontroller has a rich set of multifunctional, flexible end extended peripheral devices, it enables to elaborate a relatively simple algorithm of the measurement procedure. Hence, the code of the measurement procedure is short and satisfies the accepted condition of minimization of space occupied in the program memory.

This code consists of the main part in which Timer 0 and Timer 1 are configured to work and the parts contained in interrupt services. The services of the timers are trivial - they only stop the Timers. The code of the ADC conversion complete interrupt service occupies only two assembler instructions.

Using the interrupt system, for which each interrupt has a separate program vector in the program memory space, and using the ADC with source auto trigger by the Timer/Counter1 Overflow, it is possible to count exactly *T*, t_1, t_2 .. t_K times with the precision of a crystal oscillator without errors introduced by program delays.

3.3. The fault detection and localization procedure

The microcontroller performs the detection and the localization of single soft faults, based on the measurement results - the measurement point P_m represented by a table (a vector) of byte variables *um*[1], .., *um*[*K*] located in its RAM and the fault dictionary S_{IJ}, also in the form of a table of byte constants contained in the program memory [9].

The flowchart of the fault diagnosis function is shown in Fig. 13 [9]. It consists of two parts. In the first part the fault detection is performed. In the second one, if a fault is detected, its localization is made.

In the first fragment of the function, which deals with fault detection [9], the distance d_{nom} between the measurement point P_m and the nominal point q_{nom} is calculated and stored in a variable *d_t*. In symbolic notation *d_t* → distance(q_{nom}, P_m), the points q_{nom} and P_m represent tables of variables storing their co-ordinates remitted to the function distance. If the distance d_{nom} (the variable *d_t*) is smaller than the coefficient ε_{nom} (it is the radius of a nominal area determined by assumption of 1% tolerance of resistors and 2% tolerance of capacitors) - the measurement point P_m is inside the nominal area, which means that the tested circuit is fault-free. In this case the procedure is finished with a variable *fault* = 0. Else the microcontroller runs the fault localization part.

The fault localization fragment consists of two steps [9]. In the first step for I elements the distances d_i between l_i curves and the nominal point P_m are determined and stored in the table of byte variables $d[I]$. It is realized in the following way: at the beginning the variable $d[i]$ assumes a maximum value (d_i = FFh). Next, for each element p_i the distances d_{ij} among the point P_m and points q_{ij} representing the l_i curve are calculated in turns and simultaneously compared with the variable $d[i]$. If the particular distance d_{ij} stored in the variable *d_t* is smaller than the value of the variable $d[i]$, the value d_{ij} is written to the variable $d[i]$. In this way, using only one byte variable, the following relationship is realized by the microcontroller: $d_i = \min_{j=J}\{d_{ij}\}$.

In the second step of the fault localization fragment, the index i of the minimum distance d_i is determined and stored in the variable *fault*. So, this variable contains the number of a faulty element. In this case also only the variable *d_t* is used. It keeps the current minimum value of the distance d_i. This step can be also described in the form of the relationship: $\min_{i=1,..,I}\{d_i\} \rightarrow fault$.

This detection and the localization procedure do not depend on the number K, so it is identical for the whole class of the fault diagnosis method.

Only a distance function, which calculates the distance between two points, depends on the number K. This function bases on the following definition of the distance between two points P_1 (u_1, u_2, .., u_K) and P_2 (v_1, v_2, .., v_K):

$$d_{12} = \sum_{k=1}^{K} |u_k - v_k| \tag{19}$$

Fig. 14 shows a listing of the function distance for the 2-D method [9]. Variables x_1 and y_1 are co-ordinates of the first point, and variables x_2 and y_2 are co-ordinates of the second one. This function bases on an integer instruction: subtraction (SUB Rd,Rr), when the result is negative (the N flag is set - tested by the BRMI instruction), an one's complement (COM Rd) and an addition (ADD Rd,Rr). It is written in assembler code, so it occupies a small space (for K=2 (K=3) it consists of 13 (18) assembler instructions). Therefore it is "fast". These advantages are very important, because this function is called by the fault diagnosis procedure $I^*J + 1$ times.

After the fault diagnosis procedure, the localization results can be e.g. displayed on any display mounted in the system or they can be transmitted via the UART or the USB interface to the personal computer.

4. EXPERIMENTAL VERIFICATION

The 2-D method was experimentally verified on the example of the low-pass filter shown in Fig. 6. The analog tested part consists of an operational amplifier operating from a single power supply (V_{cc}=5V), LM158 of National Semiconductor, two resistors R1=R2=10kΩ and two capacitors C1=560pF and C2=1.1nF. It is tested by the digital part represented by the Atmega16. It works with a 6 MHz quartz crystal oscillator. Timers 0 and 1 are clocked directly by the system clock. Timer 0 generates at output OC0 stimulating square impulses with duration time T=25μs (this time corresponds to a value 0xFF – ($T_{duration} - t_{correction}$) written to Timer 0, where $T_{duration}$ = 0x96, $t_{correction}$ = 0x0A) and with an amplitude equal to V_{cc} = 5V. Times t_1 = 10μs (a value 0x36 – $t_{sample\&hold\_delay}$ loaded to Timer 1, where $t_{sample\&hold\_delay}$ = 0x2A) and t_2 = 30μs (a value 0xB4 – $t_{sample\&hold\_delay}$) are determined by the Timer 1. The ADC has the following configuration: the voltage reference is set to V_{cc}, pin ADC0 is the input channel, the result is left adjusted and the ADC is auto triggered by the interrupt from Timer 1.

In theoretical considerations and Matlab's simulations we assumed that the operational amplifier is ideal. In practice it has real parameters. So, the tested circuit was again simulated used Circuit Maker 2000 with the LM358 model. The simulation results (curves on the Fig. 15) represent the fault dictionary.

Measurements were carried out for each element change in the range from 0.1 $p_{i\ nom}$ to 10 $p_{i\ nom}$. The following values were assumed for R1 and R2 {0.1, 0.2, 0.32, 0.427, 0.51, 0.66, 0.81, 0.9, 1, 2, 3.2, 4.2, 5.1, 6.6, 7.4, 10} * 10kΩ, for C1 {0.21, 0.27, 0.32, 0.39, 0.48, 0.59, 0.7, 0.84, 1, 1.1, 3.2, 3.9} * 560pF and for C2 = {0.11, 0.14, 0.16, 0.2, 0.36, 0.43, 0.51, 0.56, 1, 1.63, 2, 4.27, 6.2, 9.1} * 1.1nF.

Different soft faults of each p_i-element were physically entered to the analog part and diagnosed on the level of fault detection and localization.

An example of experimental results is shown in Table 1. It only concerns the results of localization of C1. Table 1 shows co-ordinates of the measurement point P_m and the symbol of the element qualified as faulty.

Localization results of all elements are shown in a graphical way in Fig. 15. The curves represent theoretical calculations and single symbols represent the measurement results (measurement points).

It is seen from Table 1 and from Fig. 15 that the 2-D method for all parameter deviations gives correct results of fault localization. Only for large values of R1 a false fault localization appears two times.

5. CONCLUSIONS

In this paper, a new class of fault diagnosis methods (named *K*-D methods) for testing of analog parts of mixed-signal electronic systems and a new approach of configuration of the BISTs from internal resources of microcontrollers controlling the systems are presented. This method bases on measurements of voltage samples of the time response to a stimulating square impulse of the analog part and the fault dictionary created from the family of identification curves. The whole measurement procedure is realized only by internal resources of the microcontroller: measurements of voltage samples are realized by the ADC, the stimulating square impulse with duration time controlled by the internal timer is generated at its digital output. Detection and localisation procedures are also realized by the microcontroller using the measurement result and the fault dictionary included in its program memory.

Because this class of the fault diagnosis methods was elaborated for fault diagnosis

of analog parts of mixed signal embedded systems controlled by microcontrollers, the methods have the following advantages:

- The analog parts are measured by the reconfigurable BISTs consisting of only internal hardware resources of popular microcontrollers (timers and ADCs). Therefore it considerably decreases the cost of testing of the analog part.
- The calculations required by the diagnosis procedure are not complicated and they base on only integer instructions (subtraction, an addition and one's complement). Hence the diagnosis procedure does not require great computing power and it can be implemented in simple 8-bit microcontrollers.
- The codes of the measurement and the diagnosis procedures and the fault dictionary do not occupy much space in the program memory. So they can be added to main programs controlled the embedded microsystems without the risk of exceeding the program memory size of the microcontrollers.

So, the method can be used in practice e.g. for self-testing or automated testing of mixed-signal embedded electronic systems, or it can be also used e.g. for parametric identification of technical or biomedical objects modeled by electrical circuits.

REFERENCES

[1] Mahoney M.V.: "DSP-based testing of analogue and mixed-signal circuits", *IEEE Computer Society Press*, Siver Spring, MD, 1987.

[2] Sunter S. K., Nagi N.: "A Simplified Polynomial-Fitting Algorithm for DAC and ADC BIST" *Proc. Int. Test Conf.*, 1997, pp.389-395.

[3] Frisch A., Almy T.: "Habist: Histogram-based analogue built-in self-test", *Proc. of International Test Conference*, Washington DC, 1997, pp.760-767.

[4] Lubaszewski M., Mir S., Kolarik V., Nielsen Ch., Courtois B.: "Design of Self-Checking Fully Differential Circuits and Boards" *IEEE Transactions on Very Large Scale Integration (VLSI) Systems*, vol. 8, no. 2, April 2000, pp. 113-127.

[5] Arabi K., Kamińska B.: "Oscillation-Test Methodology for Low-Cost Testing of Active Analog Filters". *IEEE Transactions on Instrumentation and Measurement*, vol. 48, no. 4, August 1999, pp. 798-806.

[6] Toczek W., Zielonko R.: “A measuring systems for fault detection via oscillation”. *Proc. of XVI IMEKO World Congress*. Vienna, Austria, 2000, vol. 6, pp. 287-292.

[7] Toczek W.: “Analog fault signature based on sigma-delta modulation and oscillation - test methodology”. *Metrology and Measurement Systems*, 2004, Vol. XI, nr 4, pp. 363-375.

[8] Font-Rossello J., Ginard J., Isern E., Roca M., Garcia E.: “A digital bist for opamps embedded in mixed-signal circuits by analysing the transient response”. *Proc. of Forth IEEE International Caracas Conference on Devices, Circuits and Systems*, Aruba, 2002, pp. IO12-1 - IO12-5.

[9] Czaja Z.: ”About fault diagnosis methods of analog electronic circuits based on the time response to a square impulse and identification curves in multidimensional spaces“. *Proc. of Join International IMEKO TC1 + TC-7 Symposium*. Germany, Ilmenau, 2005, in CD-ROM.

[10] Czaja Z.: “Testing method of analog parts for mixed signal microsystems based on microcontrollers”, *Proc. of 13th International Symposium IMEKO TC-4*, Athens, Greece, 2004, Vol. 1, pp. 272-277.

[11] Czaja Z.: “A fault diagnosis method for analog parts of embedded systems based on time response and identification curves in the 3-D space”. *Proc. of 14th International Symposium IMEKO TC-4*. Gdynia/Jurata, Poland, 2005, vol. 2, pp. 381-386.

[12] Czaja Z., Zielonko R.: “On fault diagnosis of analogue electronic circuits based on transformations in multi-dimensional spaces”, *Measurement*, 2004, Vol. 35, No. 3, pp. 293-301.

[13] Czaja Z., Zielonko R.: “Fault diagnosis in electronic circuits based on bilinear transformation in 3D and 4D spaces”, *IEEE Trans. on Instrumentation and Measurement*, 2003, Vol. 52, No.1, pp. 97-102.

[14] Czaja Z.: „Input-output method of fault detection in analog electronic circuits taking under consideration elements’ tolerances” (In Polish: Wejściowo-wyjściowa metoda detekcji uszkodzeń w elektronicznych układach analogowych uwzględniająca tolerancje elementów). *Proc. of 3rd International Congress of Technical Diagnostics DIAGNOSTICS`2004*. September 6-9, 2004. Poznań, Poland. vol. 30 t. 1 pp. 119-122.

[15] Atmel Corporation: „8-bit AVR microcontroller with 16k Bytes In-System Programmable Flash, ATmega16, ATmega16L", PDF file, www.atmel.com, 2003.

Table 1. Measurement and localization results for the element C1

C1 [pF]	U1		U2		Faulty element
	[V]	[binary code]	[V]	[binary code]	
120	2.148	0x6E	2.949	0x97	C1
150	2.129	0x6D	2.988	0x99	C1
180	2.148	0x6E	2.832	0x91	C1
222	2.07	0x6A	3.184	0xA3	C1
271	2.051	0x69	3.32	0xAA	C1
331	1.973	0x65	3.125	0xA0	C1
391	1.836	0x5E	3.184	0xA3	C1
472	1.621	0x53	3.242	0xA6	C1
561	1.543	0x4F	3.281	0xA8	no faults
621	1.465	0x4B	3.418	0xAF	C1
1800	0.703	0x24	3.086	0x9E	C1
2200	0.703	0x24	3.066	0x9D	C1

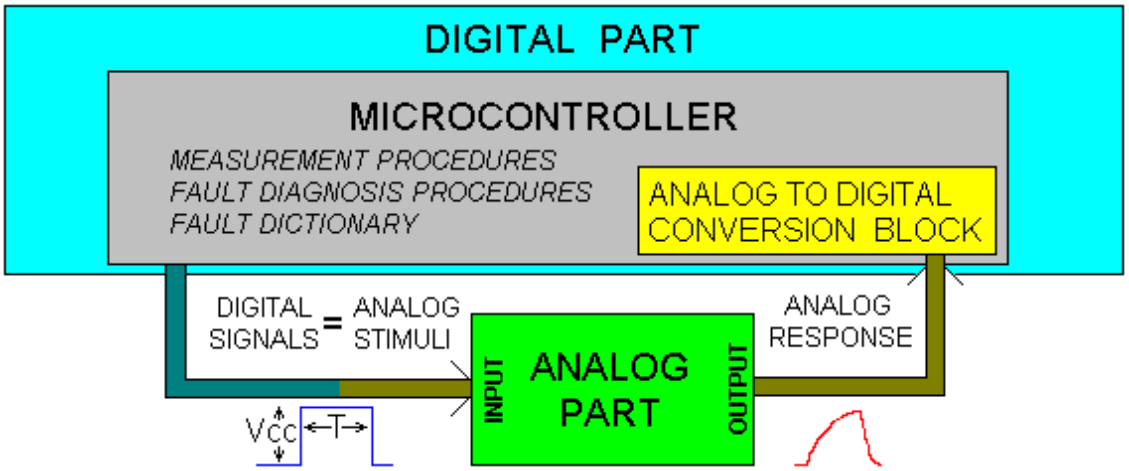

Fig. 1. An illustration of the idea of methods in the embedded system controlled by the microcontroller

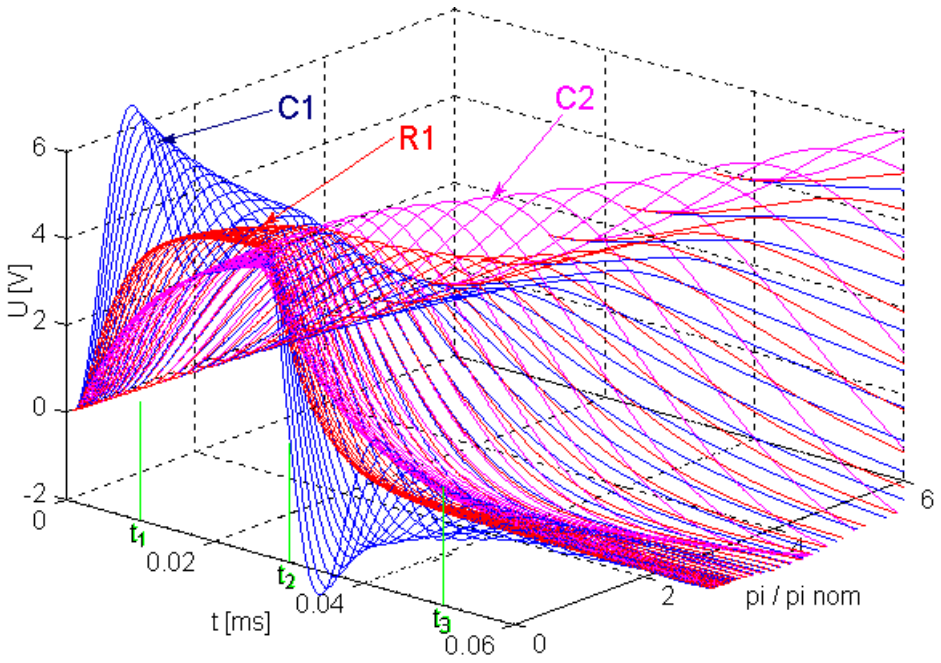

Fig. 2. Time responses of the Sallen-Key low pass filter (Fig. 6) for changes from 0.1 to 6 of nominal values of R1, C1 and C2 elements

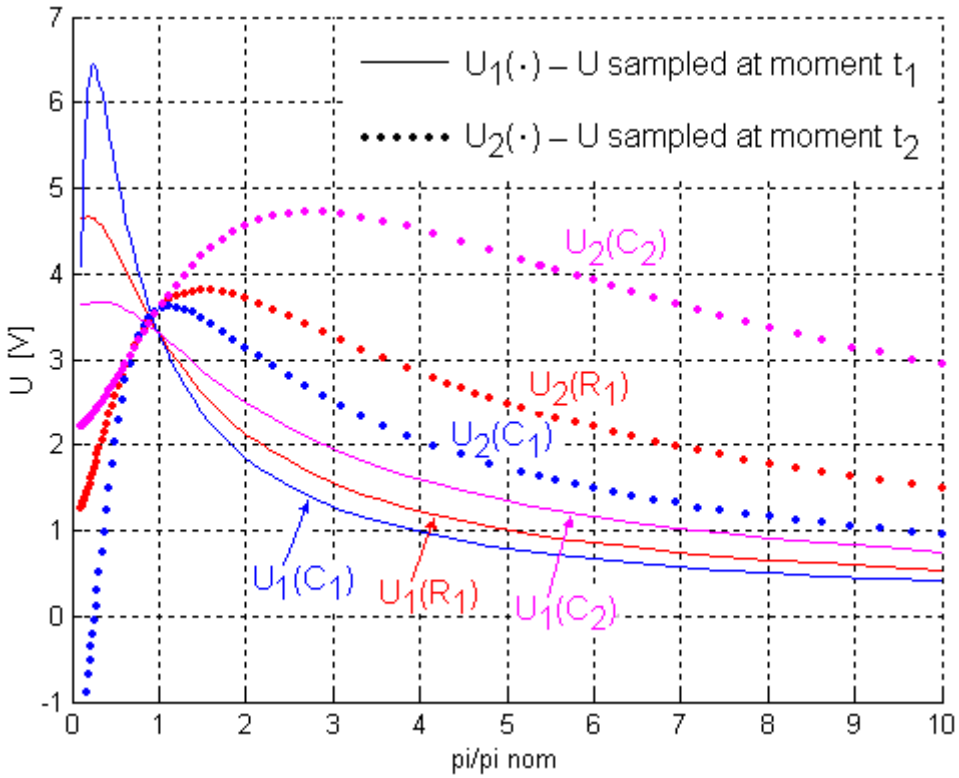

Fig. 3. Curves representing changes of values of voltage samples at moments t_1 and t_2 of time responses of the circuit in Fig. 6 in function of changes of values of elements

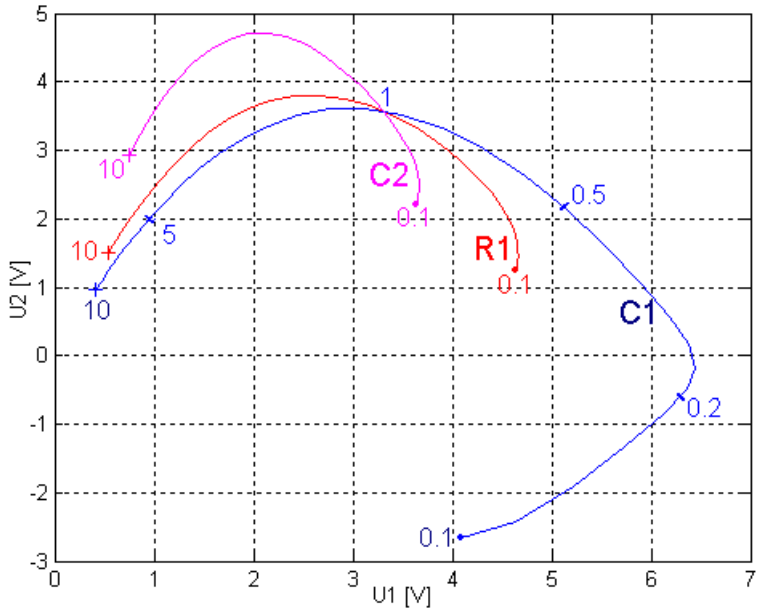

Fig. 4. Map of identification curves for the circuit (Fig. 6) for the 2-D method (K=2) for t_1 = 14.8μs and t_2 = 33.6μs

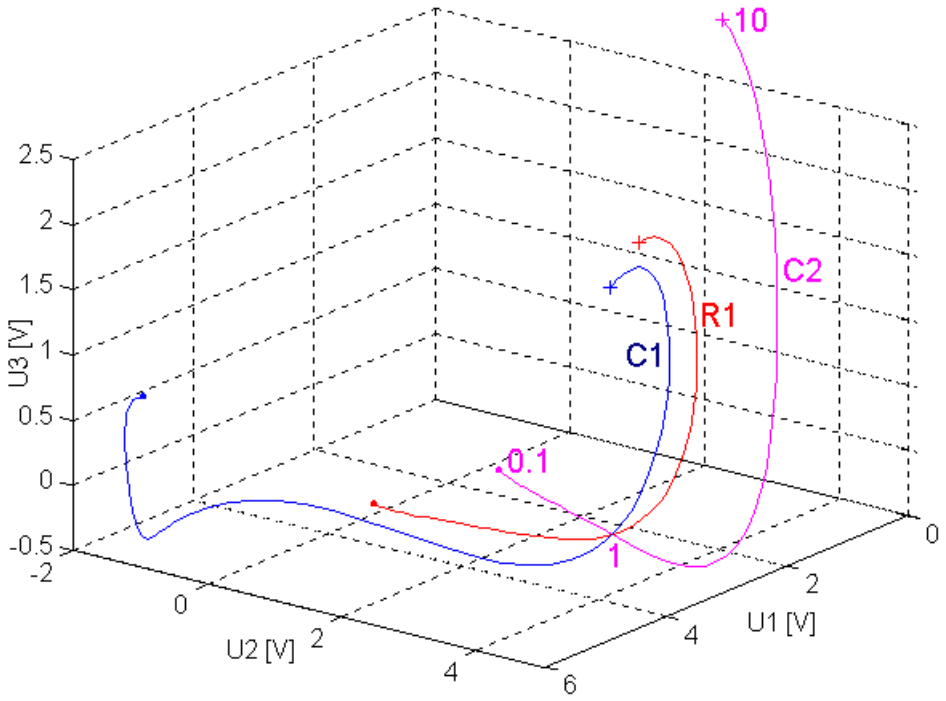

Fig. 5. Map of identification curves for the circuit (Fig. 6) for the 3-D method (K=3)

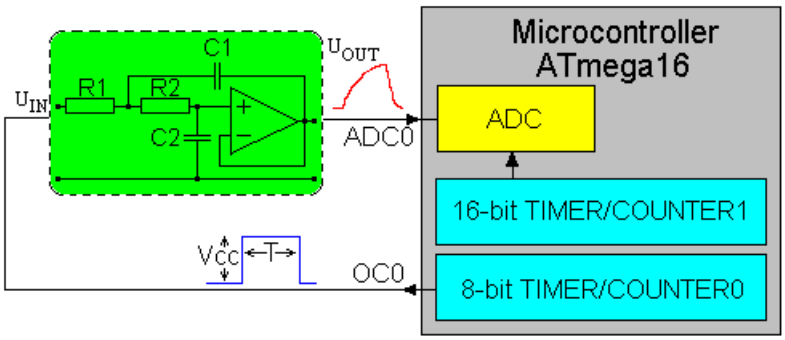

Fig. 6. Embedded system with the tested analog part, where: R1=R2=10kΩ, C1=560pF, C2=1.1nF

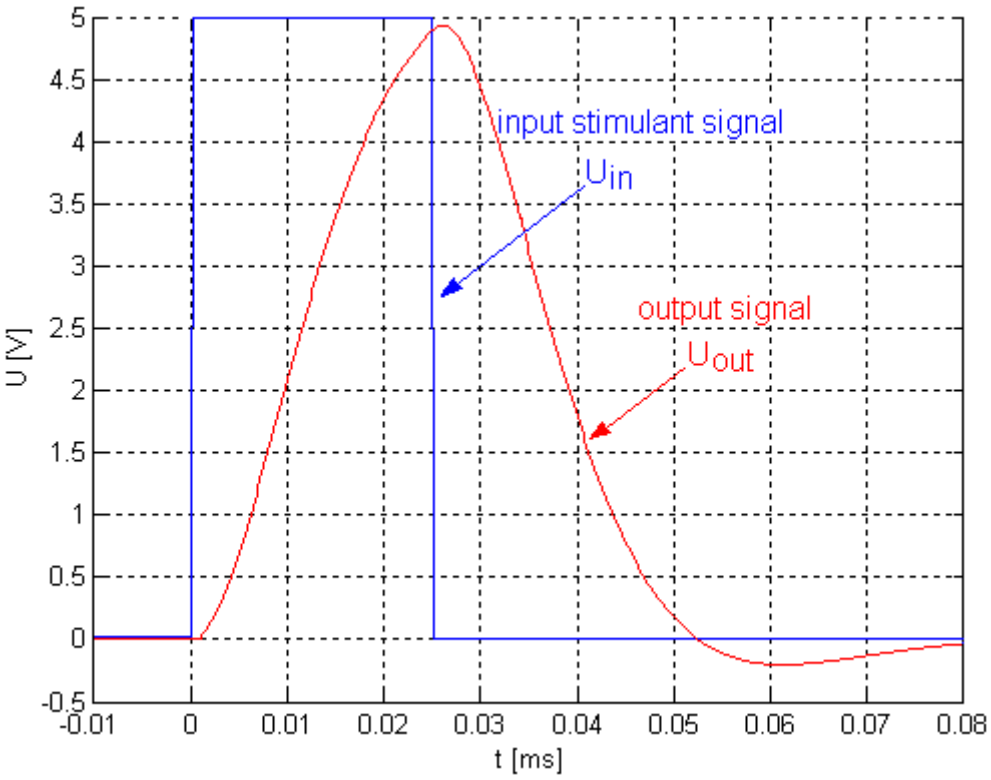

Fig. 7. The stimulating and response signals of the tested analog part (Fig. 6)

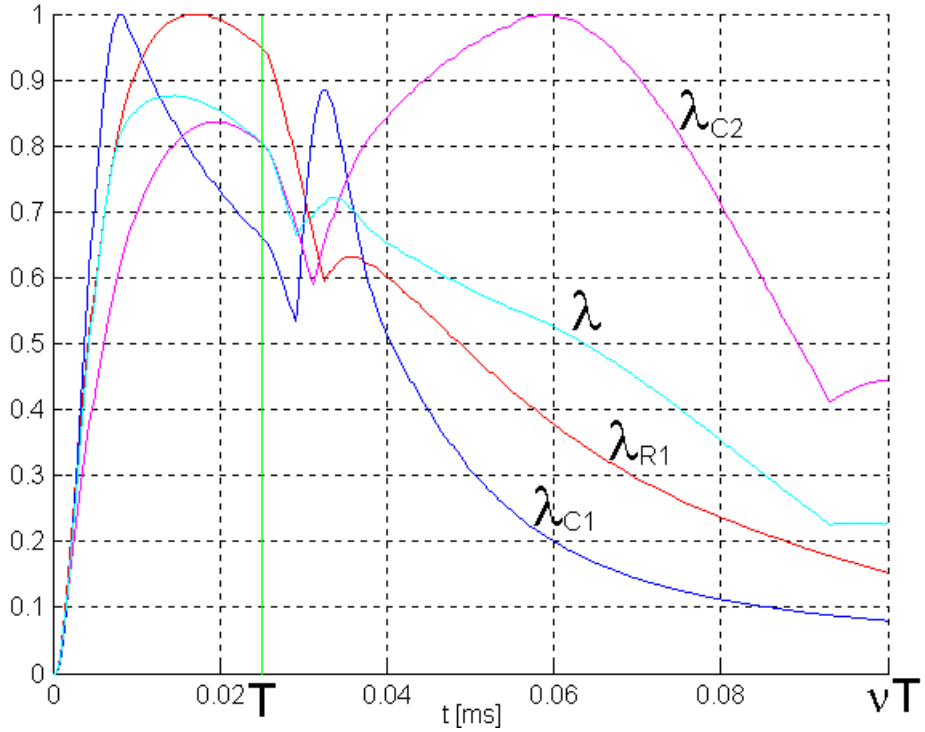

Fig. 8. Chart of the coefficient λ for the analog part of the embedded system (Fig. 6)

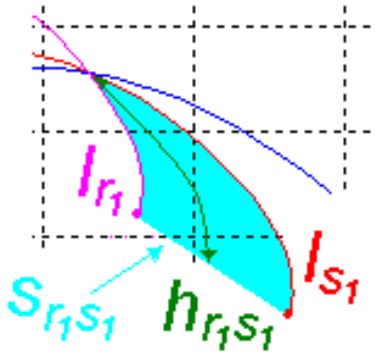

Fig. 9. Graphical interpretation of coefficients $S_{i_1^r i_1^s}$ and $l_{i_1^r i_1^s}$

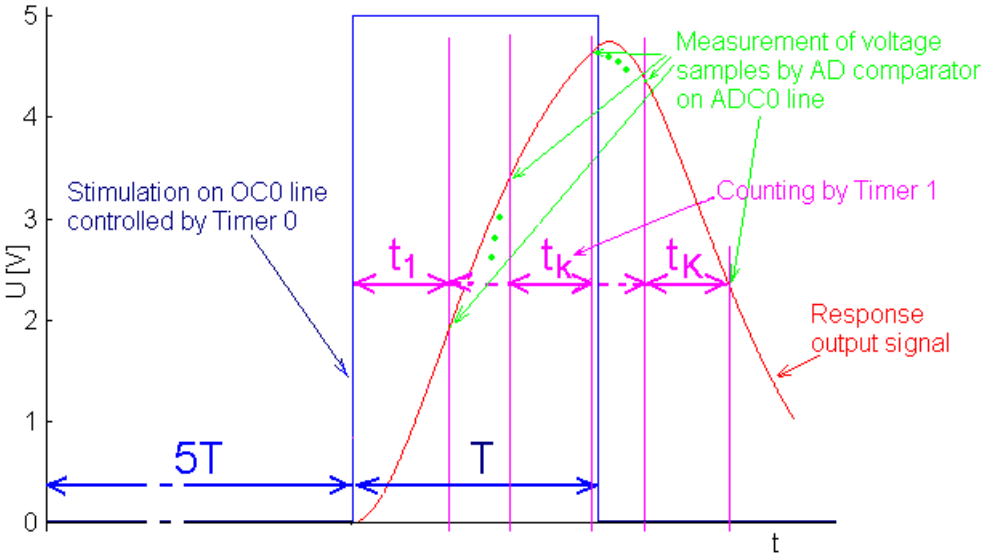

Fig. 10. The timing of the idea of the measurement procedure

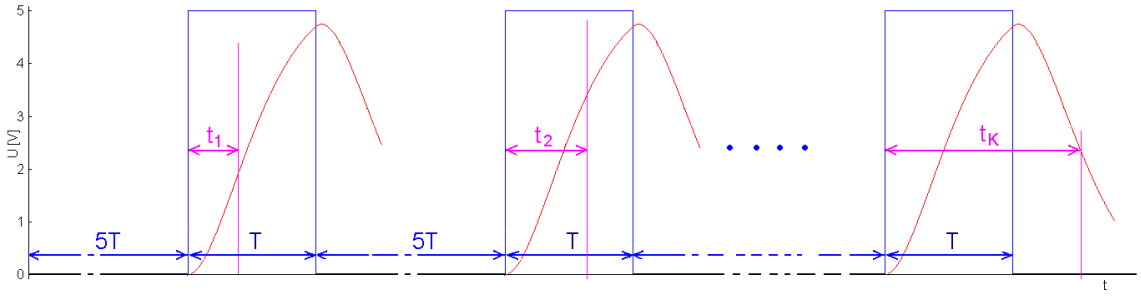

Fig. 11. The timing of the measurement procedure for *K* samples

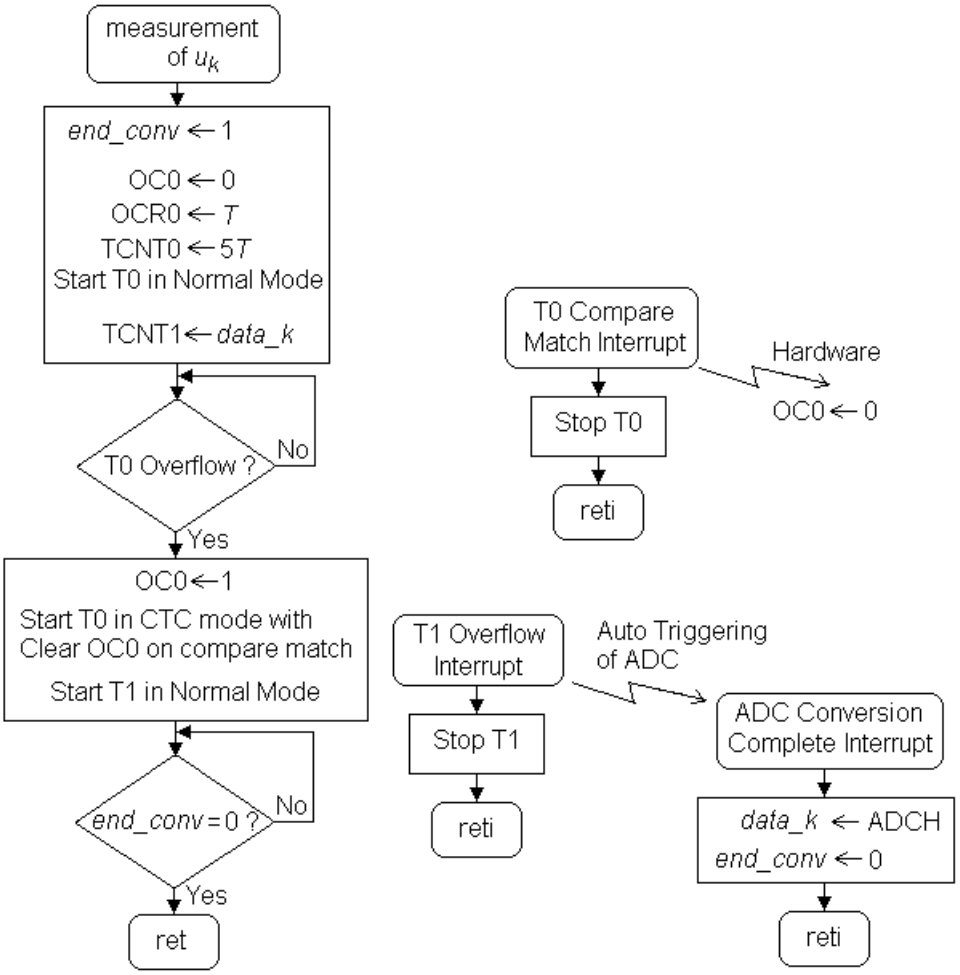

Fig. 12. The flowchart of the measurement of one sample $u_{k\,m}$ function

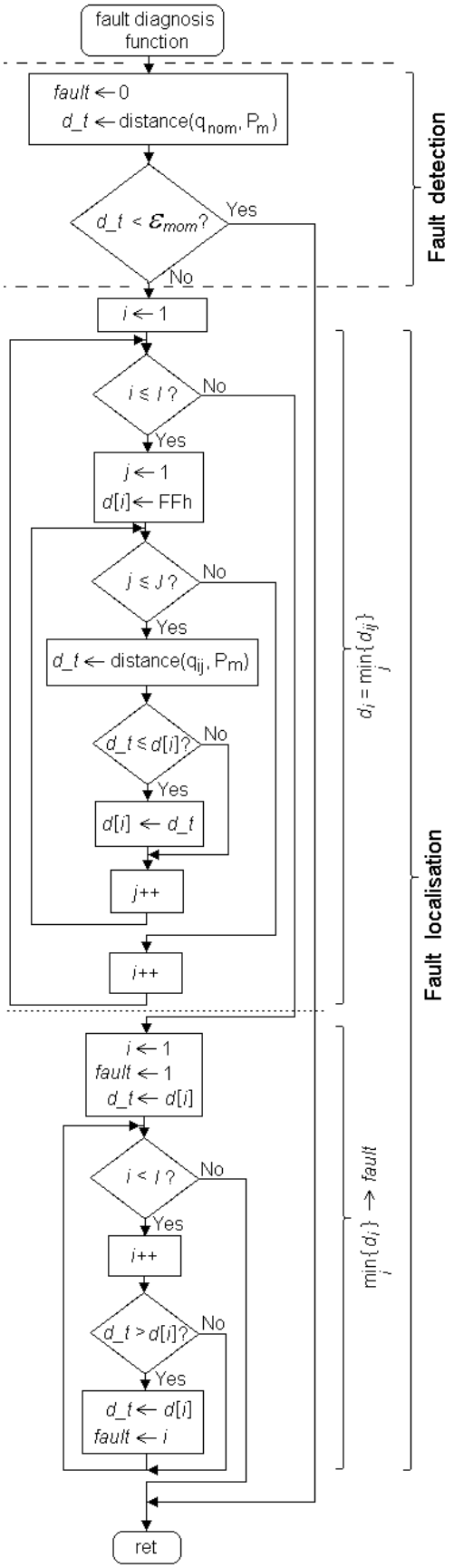

Fig. 13. Flowchart of the fault diagnosis function

```
distance:
        sub     x1,x2     ; x1 ← x1 - x2
        brpl    plusx     ; if result is minus
        com     x1        ;
        inc     x1        ; } convert to plus
plusx:                                          } Then
        sub     y1,y2     ; y1 ← y1 - y2
        brpl    plusy     ; if result is minus
        com     y1        ;
        inc     y1        ; } convert to plus
plusy:                                          } Then
        add     x1,y1     ; x1 ← x1 + x2
        brcs    carry1    ; if carry (x1 > 255)
        ret                                     } Then
carry1:
        ser x1            ; load x1 ← 0xFF
        ret
                          ; x1 contains distance d
```

Fig. 14. Listing of the function distance

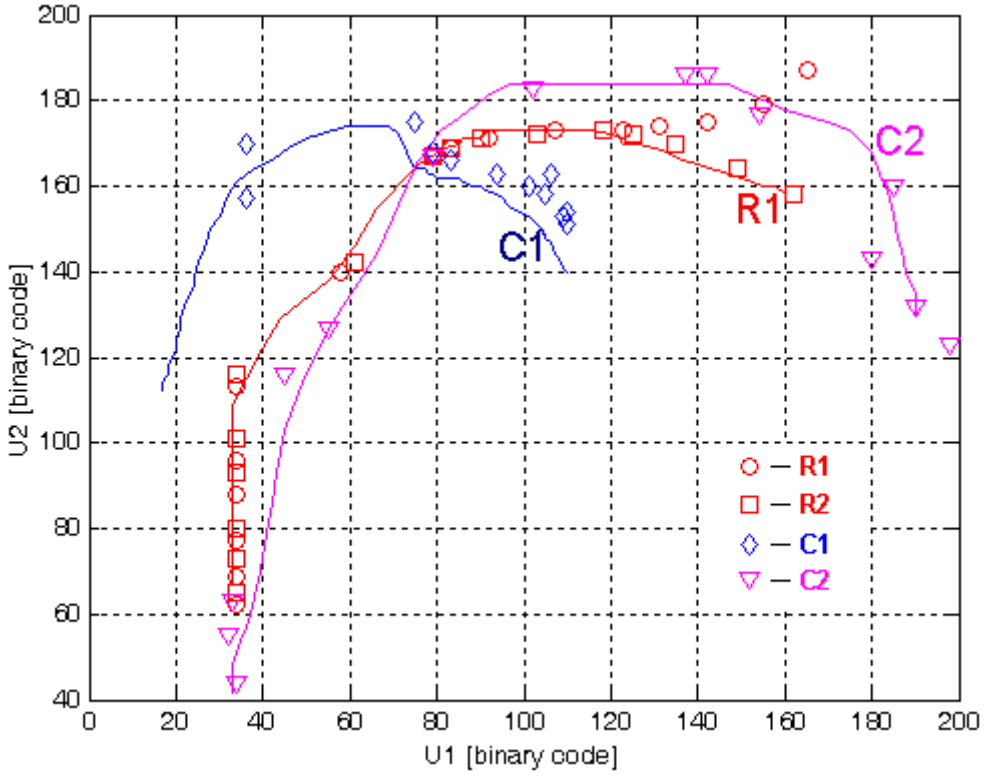

Fig. 15. Map of identification curves for the circuit (Fig. 6) for the 2-D method (t_1 = 10μs and t_2 = 30μs) together with measurement points